UC Berkeley
UC Berkeley Previously Published Works

Title

The Physics of Spin-Transfer Torque Switching in Magnetic Tunneling Junctions in Sub-10 nm Size Range

Permalink
https://escholarship.org/uc/item/5fx2r925

Journal
IEEE Transactions on Magnetics, 52(7)

ISSN
0018-9464

Authors
Hong, Jeongmin
Hadjikhani, Ali
Stone, Mark
et al.

Publication Date
2016-07-01

DOI
10.1109/tmag.2016.2530622

Peer reviewed

eScholarship.org Powered by the California Digital Library
University of California

The Physics of Spin-Transfer Torque Switching in Magnetic Tunneling Junctions in Sub-10 nm Size Range

Jeongmin Hong[1], Ali Hadjikhani[2], Mark Stone[2], Frances I. Allen[1], Vladimir Safonov[2], Ping Liang[3], Jeffrey Bokor[1], *Fellow, IEEE*, and Sakhrat Khizroev[2]

[1]Department of Electrical Engineering and Computer Sciences, University of California at Berkeley, Berkeley, CA 94720 USA
[2]Department of Electrical and Computer Engineering, Florida International University, Miami, FL 33174 USA
[3]University of California-Riverside, Riverside, CA 92521 USA

The spin-transfer torque magnetic tunneling junction (MTJ) technology may pave a way to a universal memory paradigm. MTJ devices with perpendicular magnetic anisotropy have the potential to have high thermal stability, high tunneling magnetoresistance, and low critical current for energy-efficient current-induced magnetization switching. Using devices fabricated through focused ion beam etching with Ga- and Ne-ion beams, this paper aimed to understand the size dependence of the current/voltage characteristics in the sub-10 nm range. The switching current density drastically dropped around 1 MA/cm^2 as the device size was reduced below 10 nm. A stability of over 22 kT measured for a 5 nm device indicated a significantly reduced spin relaxation time.

Index Terms—**Magnetic memory, magnetic multilayers, magnetic switching, magnetoelectronics, tunneling magnetoresistance (TMR).**

I. Introduction

SPIN-TRANSFER torque (STT) magnetic tunneling junctions (MTJs) offer the promise of a universal memory that combines the density advantage of DRAM, the speed advantage of SRAM, and the non-volatility of flash [1]–[3]. In addition, STT-MTJs can enable non-volatile logic with near zero static power consumption, meeting a key challenge in further scaling of CMOS devices. However, the relatively high energy required to switch the spin orientations in these devices remains the main stumbling block for the technology to become competitive in large market segments. Techniques, such as heat-assisted switching and voltage-controlled anisotropy, were proposed to reduce the switching current [4]. Yet, they increase the complexity of the structure and require additional power consumption for the heat source and voltage bias, respectively. We have explored the sub-10 nm regime where one can expect switching current reduction superior to that arising from linear area scaling. In this region, the thermal reservoir, which usually absorbs the energy of excitations, becomes extremely small and is unable to absorb the energy resulting from the collective spin dynamics [5]. The deviation from the crystalline lattice model in this range leads to a rapid magnetization damping decrease, which implies less energy is required for the switching. Previously, point contact experiments with a 6 nm-diameter junction indicated a switching current of approximately 90 nA, corresponding to a current density of approximately 0.1 MA/cm^2 [6]. This value is about 30 times smaller than the smallest value reported for larger size devices, on the order of 10–20 nm [7], [8]. Hence, this paper presents a comprehensive study in which MTJ devices with diameters over a wide range from sub-10 nm to over 1 μm have been fabricated using multiple focused ion beam (FIB) sources, Ga^+, Ne^+, and He^+, and tested depending on size using magnetotransport and M–H hysteresis loop measurements at room temperature.

Manuscript received November 7, 2015; revised January 17, 2016; accepted February 2, 2016. Date of publication February 18, 2016; date of current version June 22, 2016. Corresponding author: J. Hong (e-mail: jehong@berkeley.edu).

Color versions of one or more of the figures in this paper are available online at http://ieeexplore.ieee.org.

Digital Object Identifier 10.1109/TMAG.2016.2530622

II. Fabrication and Characterization

With the main focus of this paper to understand the STT effects as the device size is reduced below 10 nm, the popular Ta(5 nm)/CoFeB(1 nm)/MgO(0.9 nm)/CoFeB(1 nm)/Ta(5 nm) trilayer material composition was chosen. It is known that this composition provides an adequately high tunneling magnetoresistance (TMR) ratio, a relatively high anisotropy energy, and a relatively small switching current. The entire trilayer was fabricated through sputter deposition with an ATC 1800 ORION magnetron sputtering system from AJA International (Scituate, MA). All layers were deposited under a 10 mtorr argon processing pressure with a sample rotation rate of approximately 10 r/min to ensure complete and uniform coverage of the sample.

A perpendicular tunneling junction with a size of a few micrometers was first patterned through a standard lithographic process. Then, FIB milling from the top surface was used to trim the devices down to sizes ranging from 1 μm down to sub-10 nm. Fabrication of the larger devices was achieved by Ga-FIB milling using an FEI Quanta 3-D dual-beam FIB/SEM, whereas the smaller devices were prepared by Ne-ion milling using a Zeiss Orion NanoFab helium-ion microscope, operating the atomic source with Ne gas instead of He.

Ne- and He-ion beam microscopy is a recently developed high-resolution imaging/etching technology utilizing an atomically sharp gas field-ionization source that is useful for a variety of materials/devices applications [9], [10].

0018-9464 © 2016 IEEE. Personal use is permitted, but republication/redistribution requires IEEE permission.
See http://www.ieee.org/publications_standards/publications/rights/index.html for more information.

Advantages of He/Ne-ion lithography based on this technology compared with conventional Ga-FIB lithography using a liquid-metal source include the ability of the He/Ne beams to mill soft and fragile materials at low rates very precisely (effective probe sizes of <0.5 nm for He and <2 nm for Ne). The use of He/Ne beams in place of Ga also avoids potential negative effects of Ga implantation in the material. For the experiments presented here, small devices were fabricated choosing a Ne-ion beam instead of He due to the higher sputter yield of the heavier ion.

For the Ne milling, the Zeiss Orion NanoFab tool was operated using Ne gas at a pressure of 2×10^{-6} torr selecting a beam energy of 25 kV. Beam currents of the order of 5 pA were achieved. Milling patterns were defined using an NPVE pattern generator selecting a pixel spacing of 1 nm and a dwell time of 10 μs. Milled structures were imaged at relative low dose with the He-ion beam using an Everhart–Thornley secondary electron detector installed on the microscope. Subsequent SEM imaging was performed in the FEI dual-beam FIB/SEM tool. Cross sections through the MTJ devices for imaging by TEM were prepared by standard Ga-FIB liftout. TEM imaging was then performed using a Zeiss Libra 200MC electron microscope operated at 200 kV.

Magnetotransport measurements were performed with a lock-in amplifier with a magnetic field perpendicular to the junction plane. R–I curves were measured with Keithley meters (current source and nanovoltmeter). M–H loops were measured with a focused magneto-optical Kerr effect (MOKE) setup in the polar Kerr rotation mode.

The stability of the devices is determined through pulse applied current-induced magnetization switching (CIMS) measurements using the following equation:

$$J_C = J_{C0}[1 - (k_B T/E)\ln(\tau_p/\tau_0)] \tag{1}$$

where J_{C0} can be defined at the condition of $ln(\tau_p/\tau_0)$ to be zero and J_C can be found from linear fitting, then the stability is estimated from the slope. We assume 1 ns as τ_0 (the inverse of the attempted frequency) and actual attempted time varies from one-tenth of milliseconds up to 1 s.

III. Results

To confirm the suitable properties of the trilayer film before FIB trimming, independent sputter-deposited ferromagnetic films were studied via MOKE, as shown in Fig. 1(A). A current-in-plane TMR measurement for a pristine MTJ trilayer film before FIB trimming is shown in Fig. 1(B).

A helium-ion beam image of a typical FIB-trimmed STT-MTJ is shown in Fig. 2(A). The green dashed lines outline two islands that were formed sequentially by milling with the Ne beam. First, the upper arc was milled creating the island of size r_1. Then, after testing, a smaller island of size r_2 was created by milling the second arc. The final structure is shown in Fig. 2(B). A high-resolution TEM image of a junction trilayer cross section, obtained by Ga-FIB liftout, which confirms the designed structure of the junction, is shown in Fig. 2(C).

The smallest device measured had a planar side on the order of 5 nm. The precision of the measurement is limited

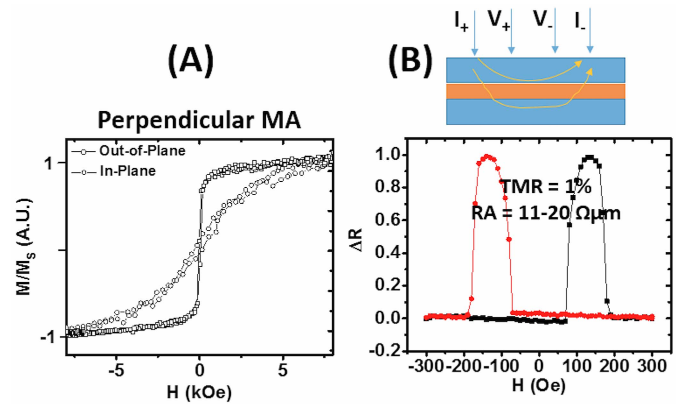

Fig. 1. (A) M–H loop of a ferromagnetic film obtained by MOKE measurement. (B) TMR effect on a pristine junction trilayer before FIB trimming measured through CIMS.

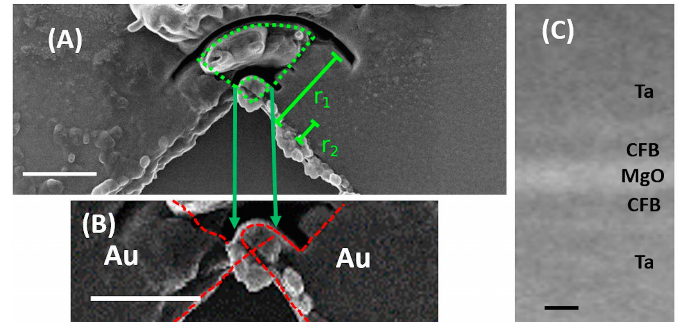

Fig. 2. (A) He-ion image of an FIB-trimmed junction. (B) Magnified view of the final island. The scale bars are 100 nm. (C) High-resolution TEM image of an MTJ junction cross section. The scale bar is 1 nm.

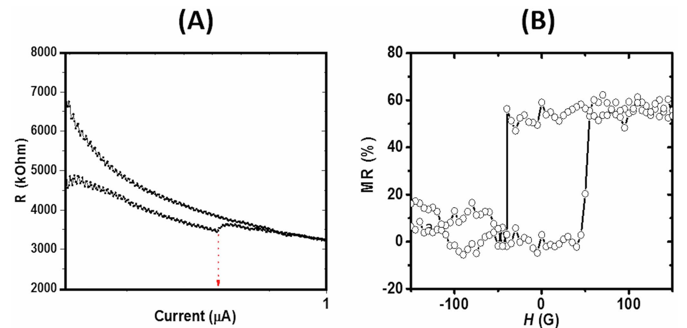

Fig. 3. (A) R–I curve of a 5 nm junction. (B) Magnetoresistance of the junction.

to about 2 nm by the SEM used to acquire the images. The size was also estimated from the resistance value which scales with the cross-sectional area. The switching current curve and the magnetoresistance for the device are shown in Fig. 3(A) and (B), respectively. The measured switching current of approximately 0.6 μA and the TMR ratio of 60% are comparable with the previously measured (through the nanoprobe technique) values of 0.1 μA and 30%, respectively, for such a small device [6].

The dependence of the measured average switching current on the effective diameter of the FIB-fabricated junction is shown with solid circular symbols in Fig. 4(A).

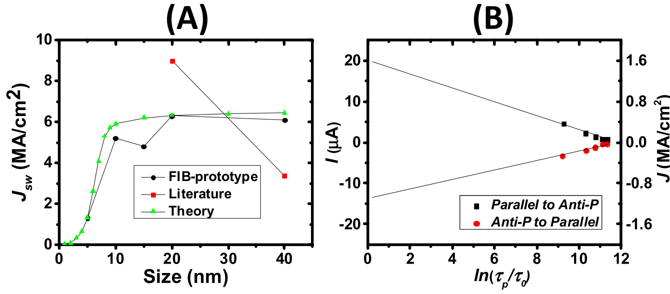

Fig. 4. (A) Size dependence of the switching current density (FIB-trimmed devices, the literature [7], [8], and theoretical curves). (B) Stability of the device.

The two red solid square symbols show the smallest switching current densities for an STT-MTJ device with a diameter above 10 nm [7], [8]. The green triangular symbols show a theoretical dependence, which was determined following the hypothesis described in the following.

IV. Discussion

According to the popular phenomenological expression by Slonczewski, the switching current density is linearly proportional to the damping constant [2]

$$J_{C0} \sim M_S t^{\alpha}/p\xi(H_{K_{\text{eff}}} \pm H_0) \quad (2)$$

where $H_{K_{\text{eff}}}$ is the anisotropy field that includes both intrinsic and shape anisotropy, H_0 is the net external field, α is the damping constant (~0.001–0.1), ξ is the spin torque efficiency factor, M_s is the saturation magnetization (~500 emu/cc), t is the thickness of the free layer (~1 nm), and p is the spin polarization, which is uniquely connected to the magnetoresistance, $\Delta R/R$, according to the Julliere equation

$$\Delta R/R = 2p^2/(1-p^2). \quad (3)$$

In general, for traditionally large device sizes (>~10 nm), the elastic modulation of exchange interaction and crystalline fields creates a coupling to phonons: L–S interactions contribute to fast and slow spin-lattice relaxation mechanisms. Spin-lattice relaxation and thermal fluctuations from the thermal reservoir destroy a Hamiltonian behavior of the spin system and, therefore, sacrifice the coherent long-lived signals. In the sub-10 nm range, it is straightforward to perform *ab initio* calculations which would directly account for all the quantum-mechanical interactions between adjacent spins [5], [6]. In this case, the spin relaxation time is expected to increase by orders of magnitude as the size is further reduced below approximately 5 nm. According to a high-level physics model [5], the effect can be described through a trivial separation of surface and volume effects; the spin relaxation time can be expressed as follows:

$$\tau_S \sim d\big/\left((1-N_S/N_V)\,\Delta g_V^2 + (N_S/N_V)\,\Delta g_S^2\right) V_F \quad (4)$$

where d is the nanostructure diameter, Δg_v and Δg_s stand for the g-factor shifts for the bulk and surface electrons, respectively, and N_v and N_s stand for the volume and surface electron concentrations, respectively. Typically, the surface shift is orders of magnitude smaller than the volume shift, Δg_v [11]. Therefore, when the size is reduced below the value at which the surface effects are dominant, the spin relaxation time could increase by orders of magnitude.

According to the results of this paper, for this particular device structure, the surface effects on the spin relaxation and, consequently, on the switching current cannot be neglected when the size is reduced below approximately 10 nm. Within the error of the experimental setup, it is difficult to give a more exact boundary value at this point. Nevertheless, from these measurements, it is clear that such a threshold boundary size is present. Above the boundary size, the device behaves according to the traditional dependence characteristic of a crystalline-type structure. Indeed, FIB-fabricated devices with a diameter above 10 nm show a switching current density comparable with that reported elsewhere in the literature. However, below the boundary size, the surface effects due to collective spin excitations become more dominant, and as a result, the spin relaxation time can be substantially increased. The latter is encouraging for STT-MTJ devices on this size scale, as shown in Fig. 4(A). For comparison, it can be noted that in this sub-10 nm size range, the traditional semiconductor devices start to display degrading properties because of the charge leakage problem [12].

When the size of any nanomagnetic device is reduced to such a small scale, the thermal stability of the device might be compromised and the term non-volatility may become relative. For example, according to a back-of-the-envelope type of evaluation, for the trilayer MTJ, in which each layer is about 1 nm thick, assuming the effective perpendicular magnetic anisotropy (K) of 10^6 J/m^3, the volume of the storage layer $V = \pi(d/2)^2 t \sim 8 \times 10^{-26}$m^3, where $d \sim 10$ nm and $t \sim 1$ nm are the diameter and thickness of the storage layer, respectively, and the thermal stability ratio, $\Delta = KV/k_BT$, at room temperature would be approximately 20. For this ratio value, the magnetic state in the storage layer would be considered thermally stable only for approximately 1 s, which is adequate only for volatile memory implementations. Note that increasing the effective anisotropy energy density only by a factor of two would increase the shelf life of the device to over ten years. Surprisingly, our measurement of an even smaller device showed a stability factor of ~22 k_BT, which indirectly confirms our hypothesis that in sub-10 nm MTJ devices, the spin relaxation increases and thus is equivalent to an effectively reduced temperature, as shown in Fig. 4(B).

V. Conclusion

In summary, we have explored relatively small STT-MTJ devices fabricated by FIB milling using multiple ion sources (Ga and Ne). We have shown that upon miniaturization in the sub-10 nm size range, the switching energy is decreased. Such device structures hold promise for high-density memory applications and logic circuits.

Acknowledgment

This work was supported in part by the National Science Foundation (NSF) under Award 0939514, in part by the U.S. Department of Energy, Office of Basic Energy Sciences,

Division of Materials Sciences and Engineering, under Contract DE-AC02-05CH11231, at the Molecular Foundry, and in part by the NSF within the Major Instrumentation Program under Grant DMR-1338139, at the Zeiss Orion NanoFab microscope, housed in the Biomolecular Nanotechnology Center/QB3 of UC Berkeley. The authors would like to thank K-Lab (www.k-lab.biz) for providing target materials and advice for the optimization of sputter deposition.

REFERENCES

[1] M. Tsoi *et al.*, "Excitation of a magnetic multilayer by an electric current," *Phys. Rev. Lett.*, vol. 80, pp. 4281–4284, May 1998.

[2] J. C. Slonczewski, "Currents and torques in metallic magnetic multilayers," *J. Magn. Magn. Mater.*, vol. 247, no. 3, pp. 324–338, 2002.

[3] L. Berger, "Emission of spin waves by a magnetic multilayer traversed by a current," *Phys. Rev. B*, vol. 54, pp. 9353–9358, Oct. 1996.

[4] A. Pushp, T. Phung, C. Rettner, B. P. Hughes, S.-H. Yang, and S. S. P. Parkin, "Giant thermal spin-torque–assisted magnetic tunnel junction switching," *Proc. Nat. Acad. Sci. USA*, vol. 112, no. 21, pp. 6585–6590, 2015.

[5] V. L. Safonov, *Nonequilibrium Magnons*. Berlin, Germany: Wiley, 2012.

[6] J. Hong, P. Liang, V. L. Safonov, and S. Khizroev, "Energy-efficient spin-transfer torque magnetization reversal in sub-10-nm magnetic tunneling junction point contacts," *J. Nanoparticle Res.*, vol. 15, no. 4, pp. 1–6, 2013.

[7] S. Ikeda *et al.*, "A perpendicular-anisotropy CoFeB–MgO magnetic tunnel junction," *Nature Mater.*, vol. 9, pp. 721–724, Sep. 2010.

[8] M. Gajek *et al.*, "Spin torque switching of 20 nm magnetic tunnel junctions with perpendicular anisotropy," *Appl. Phys. Lett.*, vol. 100, no. 13, p. 132408, 2012.

[9] S. Tan *et al.*, "Nanomachining with a focused neon beam: A preliminary investigation for semiconductor circuit editing and failure analysis," *J. Vac. Sci. Technol. B*, vol. 29, no. 6, p. 06F604, 2011.

[10] G. Hlawacek, V. Veligura, R. van Gastel, and B. Poelsema, "Helium ion microscopy," *J. Vac. Sci. Technol. B*, vol. 32, no. 2, p. 020801, 2014.

[11] J. C. Slonczewski, "Conductance and exchange coupling of two ferromagnets separated by a tunneling barrier," *Phys. Rev. B*, vol. 39, no. 10, p. 6995, 1989.

[12] J. D. Meindl, Q. Chen, and J. A. Davis, "Limits on silicon nanoelectronics for terascale integration," *Science*, vol. 293, no. 5537, pp. 2044–2049, Sep. 2001.